Biochemical and Biophysical Research Communications 424 (2012) 52–57

Contents lists available at SciVerse ScienceDirect

Biochemical and Biophysical Research Communications

journal homepage: www.elsevier.com/locate/ybbrc

Cytochalasin D acts as an inhibitor of the actin–cofilin interaction

Kazuyasu Shoji [a,b], Kazumasa Ohashi [a,b], Kaori Sampei [a], Masato Oikawa [c], Kensaku Mizuno [a,b,*]

[a] Department of Biomolecular Sciences, Graduate School of Life Sciences, Tohoku University, Sendai, Miyagi 980-8578, Japan
[b] Department of Biology, Graduate School of Science, Tohoku University, Sendai, Miyagi 980-8578, Japan
[c] Graduate School of Nanobioscience, Yokohama City University, Seto, Kanazawa-ku, Yokohama 236-0027, Japan

ARTICLE INFO

Article history:
Received 12 June 2012
Available online 20 June 2012

Keywords:
Cytochalasin D
Cofilin
Actin dynamics
Inhibitor
Protein–protein interaction
Bimolecular fluorescence complementation (BiFC)

ABSTRACT

Cofilin, a key regulator of actin filament dynamics, binds to G- and F-actin and promotes actin filament turnover by stimulating depolymerization and severance of actin filaments. In this study, cytochalasin D (CytoD), a widely used inhibitor of actin dynamics, was found to act as an inhibitor of the G-actin–cofilin interaction by binding to G-actin. CytoD also inhibited the binding of cofilin to F-actin and decreased the rate of both actin polymerization and depolymerization in living cells. CytoD altered cellular F-actin organization but did not induce net actin polymerization or depolymerization. These results suggest that CytoD inhibits actin filament dynamics in cells via multiple mechanisms, including the well-known barbed-end capping mechanism and as shown in this study, the inhibition of G- and F-actin binding to cofilin.

1. Introduction

Actin filament dynamics play an essential role in numerous cell activities, including migration, morphological changes and division. Among actin-binding proteins, cofilin is a key regulator of actin filament dynamics and reorganization [1–4]. It binds to both G- and F-actin and promotes actin filament turnover by stimulating depolymerization and severance of actin filaments [1–4]. The actin-binding activity of cofilin is inactivated upon phosphorylation of its Ser-3 residue by LIM-kinases or related TESK kinases [5–7], and reactivated upon dephosphorylation by the Slingshot family of protein phosphatases [8,9]. The actin–cofilin interaction is also negatively regulated upon binding of phosphoinositides, such as phosphatidylinositol 4,5-bisphosphate (PIP2), to cofilin [10], and upon binding of actin-binding proteins, such as profilin and tropomyosin, to G- or F-actin [11–13].

Cytochalasin D (CytoD) is a fungus-derived small organic compound that is widely used for investigating the role of actin dynamics in cellular processes [14]. CytoD binds to the barbed ends of actin filaments with high affinity (Kd; ~2 nM) and inhibits both the polymerization and depolymerization of actin subunits at this end [14–16]. CytoD also binds to G-actin with low affinity (Kd; 2–20 μM) and induces actin dimer formation, which can lead to the nucleation of new filaments [14,17,18]. CytoD binding to G-actin may affect the interaction between G-actin and G-actin-binding proteins [19]. In cells, CytoD has multiple effects on actin dynamics, depending on the CytoD concentration used and the cellular concentrations of G-actin, actin filament free barbed ends, ATP and various actin-binding proteins [14]. For example, CytoD inhibited actin polymerization and induced actin filament depolymerization in thrombin-stimulated platelets [20], whereas it did not produce net depolymerization of actin filaments in HEp-2 tumor cells [21]. Hence, despite the widespread use of CytoD, its mechanism of action is still not fully understood.

We recently developed the bimolecular fluorescence complementation (BiFC) assay to detect the interaction between G-actin and cofilin [22]. This assay is based on the reassembly of Venus, a variant of YFP [23], from its nonfluorescent fragments, which is mediated by the interaction between two proteins of interest fused to each fragment [24]. Using the *in vitro* BiFC assay, we searched for inhibitors of the G-actin–cofilin interaction and identified CytoD. Our results indicate that CytoD affects intracellular actin cytoskeletal dynamics via multiple mechanisms, including the inhibition of G- and F-actin binding to cofilin.

Abbreviations: BiFC, bimolecular fluorescence complementation; CBB, coomassie brilliant blue; CytoD, cytochalasin D; FDAP, fluorescence decay after photoactivation; FRAP, fluorescence recovery after photobleaching; YFP, yellow fluorescent protein.

* Corresponding author at: Department of Biomolecular Sciences, Graduate School of Life Sciences, Tohoku University, Sendai, Miyagi 980-8578, Japan. Fax: +81 22 795 6678.
E-mail address: kmizuno@biology.tohoku.ac.jp (K. Mizuno).

0006-291X/$ - see front matter © 2012 Elsevier Inc. All rights reserved.
http://dx.doi.org/10.1016/j.bbrc.2012.06.063

2. Materials and methods

2.1. Materials

The SCADS inhibitor kit I and II (each consisting 95 chemical inhibitors) were provided by the Screening Committee of Anticancer Drugs through a Grant-in-Aid for Scientific Research on Priority Area 'Cancer' from the Ministry of Education, Culture, Sports, Science and Technology, Japan. Other chemical compounds (termed MO-1 to MO-768) had been synthesized as partial structures and analogs of natural products as well as enzyme inhibitors [25–27].

2.2. Plasmid construction

The Venus and Dronpa cDNA constructs were provided by A. Miyawaki (Riken, Wako, Japan) [23,28]. The generation of the expression plasmids encoding the His_6-tagged BiFC probes, actin-VC210 (the *C*-terminal fragment 210–238 of Venus fused to the *C*-terminus of actin) and VN210-cofilin (the *N*-terminal fragment 1-210 of Venus fused to the *N*-terminus of cofilin), was described previously [22].

2.3. Cell culture and transfection

COS-7 cells were cultured in Dulbecco's modified Eagle's medium (DMEM) supplemented with 10% fetal calf serum. Cells were transfected with expression plasmids using Lipofectamine 2000 (Invitrogen).

2.4. Screening of inhibitors

Screening of inhibitors of the G-actin–cofilin interaction was performed using the *in vitro* BiFC assay with probes composed of actin-VC210 and VN210-cofilin, as described previously [22]. His_6-tagged actin-VC210 and VN210-cofilin were expressed in Sf9 cells, using the Bac-to-Bac baculovirus expression system (Invitrogen). Proteins were passed through a nickel–nitrilotriacetic acid agarose (Qiagen) column, eluted with 0.2 M imidazole buffer and subjected to gel-filtration using a PD-10 column (GE Healthcare) to exchange the imidazole buffer for binding buffer [22]. The actin-VC210 (1.5 μM) and VN210-cofilin (3 μM) probes were incubated with each small organic compound at final concentrations of 6.6 and 10 μM at 30 °C in 96-well microtiter plates. Fluorescence intensity was measured at 0 and 120 min at 545 nm with excitation at 505 nm in a fluorescence microphotometer. The experiments were done using duplicate samples.

2.5. F-actin sedimentation assay

The F-actin cosedimentation assay was performed as described previously [8,9]. Rabbit skeletal muscle actin was polymerized and incubated with various concentrations of CytoD in the presence or absence of His_6-tagged cofilin purified from Sf9 cells.

2.6. Fluorescence recovery after photobleaching (FRAP) and fluorescence decay after photoactivation (FDAP) assays

FRAP and FDAP analyses were performed as described previously [29–31]. COS-7 cells transfected with YFP-actin or Dronpa-actin were cultured in DMEM containing 10 mM Hepes (pH 7.4) and 10% fetal calf serum at 37 °C and exposed to CytoD or control vehicle (DMSO) for 30 min. Cells were then subjected to FRAP or FDAP analysis using a laser-scanning confocal microscope (LSM 510; Carl Zeiss) equipped with a PL Apo 63× oil-immersion objective lens (NA 1.4). For FRAP analysis, prior to photobleaching, a fluorescence image of the cell in a rectangular region (104.4 × 61.2 μm) was acquired by irradiation with a 514 nm argon-ion laser under low power. Photobleaching was performed in a region (67.3 × 6.1 μm) by irradiation with the full power of a 30 mW argon-ion laser at 458, 488 and 514 nm for 1.9 s. Immediately after photobleaching, fluorescence images were acquired every 1 s for 60 s by weak irradiation with a 514 nm laser. The fluorescence intensity of a rectangular region (20.4 × 6.1 μm) within the photobleached area was measured and normalized to the value before photobleaching. For FDAP analysis, after photobleaching the whole cell by intense irradiation with a 488 nm laser, Dronpa-actin was photoactivated in a rectangular region (78.5 × 7.1 μm) by intense irradiation with a 458 nm laser for 2.8 s. Immediately after photoactivation, fluorescence images were acquired every 1 s for 40 s by weak irradiation with the 488 nm laser. The fluorescence intensity of the F-actin-rich region within the photoactivated area was measured and normalized to the value immediately after photoactivation. A photobleaching correction was performed by measuring the fluorescence decay of Dronpa-actin in the whole cell under the same conditions.

3. Results

3.1. Identification of CytoD as an inhibitor of the actin–cofilin interaction

To search for inhibitors of the actin–cofilin interaction, the *in vitro* BiFC assay system, in which inhibitors of the actin–cofilin interaction are expected to inhibit the fluorescence recovery of BiFC probes composed of actin-VC210 and VN210-cofilin, was used (Fig. 1A). His_6-tagged actin-VC210 and VN210-cofilin proteins were individually expressed in Sf9 cells and purified, and then a library of low molecular weight compounds (including 209 known inhibitors, three natural compounds, and 746 chemically synthesized compounds) was screened to identify compounds with the ability to inhibit fluorescence recovery from the pair of BiFC probes. Of 958 compounds screened, CytoD markedly inhibited fluorescence recovery reproducibly and four other compounds (NSC95397, Sanguinarin, GS416 and MO-345) moderately inhibited fluorescence recovery, while the other compounds failed to inhibit recovery (Fig. 1B). These five compounds were tested for their ability to inhibit the interaction between active H-Ras and the Ras-binding domain (RBD) of Raf1 [22] using the RasV12-VC210 and VN210-Raf1(RBD) BiFC probes. NSC95397, Sanguinarin, GS416 and MO-345, but not CytoD, inhibited fluorescence recovery (data not shown), suggesting that CytoD inhibits the interaction between actin and cofilin specifically, while the other four compounds likely inhibit the interaction between the Venus fragments.

3.2. CytoD inhibits the actin–cofilin interaction by binding to G-actin

The effect of CytoD on the time-dependent fluorescence recovery of the actin-VC210 and VN210-cofilin probe pair was assessed over a range of CytoD concentrations. CytoD suppressed the recovery of Venus fluorescence at concentrations greater than 1 μM (Fig. 1C). To determine whether CytoD inhibits the actin–cofilin interaction by binding to G-actin or cofilin or both, we assessed the effect of 1.5 μM CytoD on fluorescence recovery of the pair of 1.5 μM actin-VC210 and 10 μM VN210-cofilin or the pair of 1.5 μM VN210-cofilin and 10 μM actin-VC210. As shown in Fig. 1D, 1.5 μM CytoD almost completely inhibited the fluorescence recovery observed with 1.5 μM actin-VC210 and 10 μM VN210-cofilin, but not that observed with 1.5 μM VN210-cofilin and 10 μM actin-VC210, indicating that the inhibitory effect of CytoD was abrogated by excess amounts of the actin probe but not by

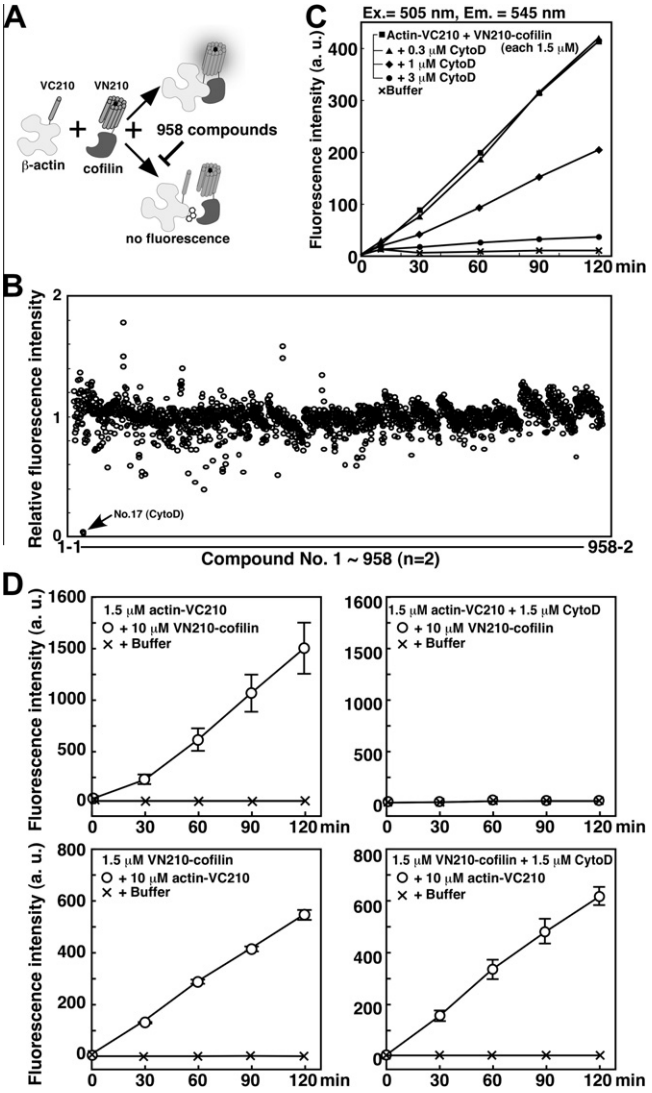

Fig. 1. Identification of CytoD as an inhibitor of the G-actin–cofilin interaction. (A) Schematic diagram of the BiFC assay used for inhibitor screening. (B) Screening of inhibitors of the G-actin–cofilin interaction. The actin-VC210 and VN210-cofilin probe pair was incubated with a library of chemical compounds. The relative fluorescence intensity recovered is shown and compared to the value of control reactions without addition of compound. (C) Inhibitory effect of CytoD on the G-actin–cofilin interaction. The time-dependent fluorescence recovery of the BiFC probes was measured in the presence of indicated concentrations of CytoD. (D) CytoD inhibits the G-actin–cofilin interaction by binding to G-actin. The effect of 1.5 μM CytoD on the fluorescence recovery observed with 1.5 μM actin-VC210 and 10 μM VN210-cofilin or with 1.5 μM VN210-cofilin and 10 μM actin-VC210 was measured as in (C). a.u., arbitrary unit.

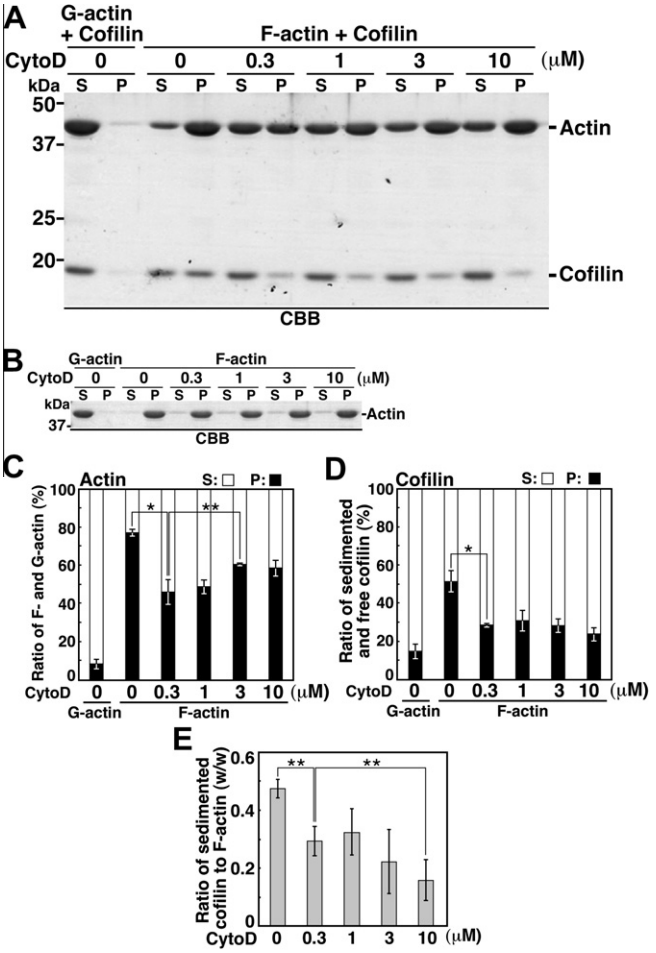

Fig. 2. CytoD inhibits the binding of F-actin to cofilin. (A and B) F-actin sedimentation assay. F-actin polymerized from 4 μM of G-actin was incubated for 30 min with CytoD in the presence (A) or absence (B) of 2 μM cofilin and then ultracentrifuged. Equal portions of the pellets (P) and the supernatants (S) were subjected to SDS–PAGE and analyzed by CBB staining. (C) Quantification of the ratio of F-actin (in the pellets) and G-actin (in the supernatants) to total actin. (D) Quantification of the ratio of cosedimented cofilin (in the pellets) and free cofilin (in the supernatants) to total cofilin. (E) Quantification of the ratio of cofilin to F-actin in the pellets. From (C) to (E), data represent means ± S.D. of triplicate experiments. *, $p < 0.01$; **, $p < 0.05$.

excess amounts of the cofilin probe, thereby demonstrating that CytoD inhibits the G-actin–cofilin interaction by binding to G-actin.

3.3. CytoD inhibits the binding of F-actin to cofilin

Like cofilin, CytoD also binds to both G- and F-actin. Therefore, we next assessed the effect of CytoD on actin polymerization and on the cofilin-binding ability of F-actin by *in vitro* F-actin sedimentation assays. Polymerized actin was incubated with various concentrations of CytoD in the presence or absence of cofilin and ultracentrifuged at 100,000*g* to precipitate F-actin (Figs. 2A and B). The amounts of F-actin and G-actin recovered in the pellet and the supernatant respectively and the amounts of cofilin cosedimented and not cosedimented with F-actin were measured by densitometric analysis of a CBB-stained gel. CytoD did not affect the ratio of F-actin to total actin (G- plus F-actin) in the absence of cofilin (Fig. 2B). In contrast, CytoD significantly decreased the ratio of F-actin to total actin in the presence of cofilin (Figs. 2A and C); the percentage of F-actin was 77% in the absence of CytoD, 46% in the presence of 0.3–1 μM CytoD and 59–61% in the presence of 3–10 μM CytoD (Fig. 2C). These results indicate that, in the presence of cofilin, a low concentration of CytoD effectively reduces the F-actin ratio, probably by capping the barbed ends of actin filaments, whereas at higher concentrations, CytoD tends to increase the F-actin ratio, probably by weakening the interaction between F-actin and cofilin. The ratio of cofilin in the pellet fraction to total cofilin was reduced in the presence of CytoD (Fig. 2D). Furthermore, the ratio of cofilin to F-actin in the pellet was reduced in the presence of CytoD, with maximum reduction detected at 10 μM CytoD (Fig. 2E). These results indicate that CytoD inhibits the binding of F-actin to cofilin.

3.4. Effect of CytoD on actin dynamics in cultured cells

To examine the effect of CytoD on cellular actin dynamics, COS-7 cells were exposed to various concentrations of CytoD for 30 min and the ratio of F-actin to total actin was analyzed by sedimentation analysis (Fig. 3A). The ratio of F-actin to total actin did not significantly change upon exposure to CytoD at concentrations ranging from 0.3 to 10 μM (Fig. 3B). When the effect of CytoD on cellular F-actin was analyzed by phalloidin staining, no apparent change was observed at concentrations ranging from 0.3 to 1 μM, but retraction and arborization of the cell and conversion of F-actin from long fibers to punctate structures were observed at concentrations ranging from 3 to 10 μM (Fig. 3C).

The effect of CytoD on F-actin dynamics was then examined in living cells by FRAP and FDAP analysis. For FRAP analysis, COS-7 cells expressing YFP-actin were exposed to CytoD for 30 min, and then YFP-actin fluorescence in the F-actin-rich peripheral region of the cell was photobleached and fluorescence recovery was monitored every second for 60 s (Figs. 4A and B). CytoD significantly decreased the rate of fluorescence recovery in a concentration-dependent manner (Fig. 4B), indicating that CytoD decreases the rate of actin polymerization in living cells. The effect of CytoD on the rate of actin depolymerization was also examined by FDAP analysis. COS-7 cells expressing Dronpa-actin were exposed to CytoD for 30 min. After photobleaching the whole cell, Dronpa-actin fluorescence was photoactivated in the F-actin-rich peripheral region of the cell. Fluorescence images were acquired every second for 40 s (Figs. 4C and D). CytoD decreased the rate of Dronpa-actin fluorescence delay in a concentration-dependent manner (Fig. 4D), indicating that CytoD decreases the rate of actin depolymerization in cells.

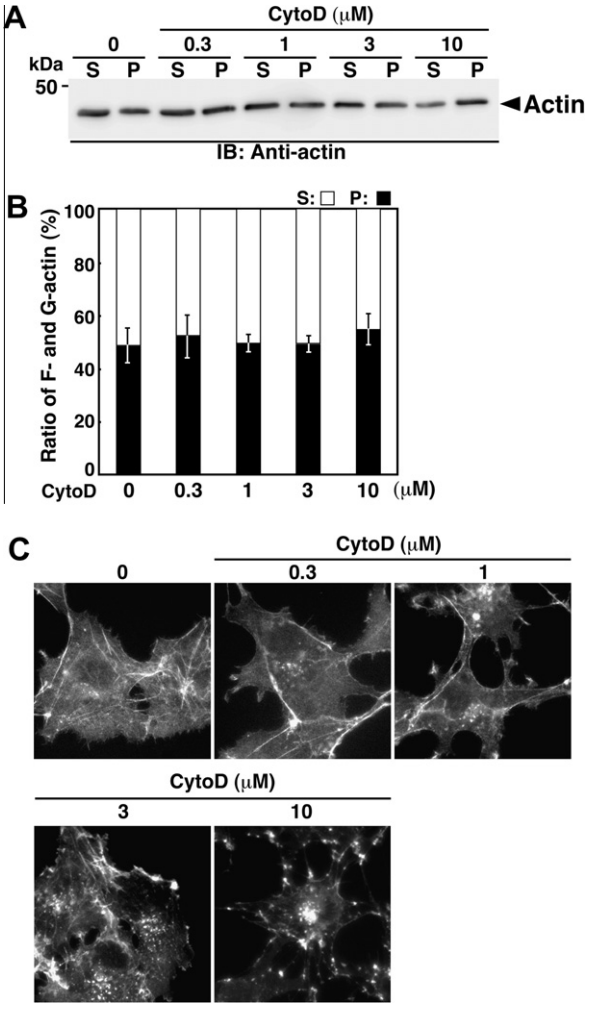

Fig. 3. Effect of CytoD on the cellular F-actin ratio and F-actin organization. (A) Effect of CytoD on the cellular F-actin ratio. COS-7 cells were exposed to CytoD for 30 min and then the cell lysates were centrifuged at 100,000*g* for 30 min. The amounts of F-actin and G-actin in the precipitates (P) and supernatants (S) were analyzed by immunoblotting with anti-actin antibody. (B) Quantification of the ratio of F- and G-actin to total actin. Data represent means ± S.D. of triplicate experiments. No significant change was detected. (C) Effect of CytoD on F-actin organization and cell morphology. COS-7 cells were exposed to CytoD for 30 min, fixed and stained with rhodamine–phalloidin. Scale bar, 20 μm.

4. Discussion

This study identified CytoD as an inhibitor of the G-actin–cofilin interaction using the BiFC assay system recently developed in our laboratory [22]. The BiFC assay, which employs a pair of Venus fragments obtained by splitting the Venus protein at position 210, can detect protein-protein interactions with high specificity and low background fluorescence [22]. It is therefore ideal for the screening of inhibitors of a wide range of protein–protein interactions.

CytoD inhibits the G-actin–cofilin interaction by binding to G-actin. Previous studies showed that CytoD binds to G-actin [17–19]. Crystal structure analysis of the CytoD–G-actin complex showed that CytoD binds to G-actin via the hydrophobic cleft between subdomains 1 and 3 at the barbed end of G-actin [19], which is the same region involved in G-actin binding to cofilin [32–35]. Thus, it is likely that CytoD inhibits the G-actin–cofilin interaction by competing with cofilin for binding to this hydrophobic cleft of G-actin. Since several actin-targeting toxins, such as trisoxazole and bistramide A, also bind to this hydrophobic cleft of G-actin [36], these toxins may also inhibit the actin–cofilin interaction. In addition, the CytoD-binding cleft in actin overlaps with the binding site of several G-actin-binding proteins, including profilin, vitamin D-binding protein and the Wiskott–Aldrich syndrome protein-homology 2 (WH2) domain of Ciboulot [35]. Thymosin-β4 is also predicted to bind to G-actin through this cleft [37]. A large pool of cellular G-actin is complexed with thymosin-β4, profilin and cofilin [3]. Since these G-actin-binding proteins perform regulatory roles in actin dynamics by sequestering G-actin (thymosin-β4 and cofilin) and promoting actin assembly at the barbed end (profilin), CytoD may affect cellular actin dynamics by competing with these actin-binding proteins for binding to G-actin.

F-actin sedimentation experiments revealed that CytoD significantly decreased the ratio of F-actin to total actin in the presence of cofilin (Fig. 2C). This is probably caused by CytoD capping of the barbed ends of actin filaments, together with the actin-depolymerizing and -severing activity of cofilin near the pointed end. Interestingly, CytoD also decreased the ratio of cofilin to F-actin in the pellet fraction (Fig. 2E), indicating that CytoD can inhibit the binding of cofilin to F-actin. Considering that CytoD binds to the barbed ends of actin filaments with a stoichiometry of about one CytoD molecule per filament [14,15], CytoD binding to the barbed end of F-actin may inhibit F-actin binding to cofilin by altering the structural organization of the whole filament so that it becomes inaccessible to cofilin. In this respect, a previous study showed that barbed-end capping by CytoD inhibits the bursting disassembly of actin filaments induced by cofilin, coronin and actin-interacting protein 1 (Aip1) [38]. Thus, it is possible that the binding of CytoD to the barbed ends of actin filaments not only inhibits actin polymerization and depolymerization at barbed ends but also inhibits cofilin-mediated actin filament disassembly along the whole actin filament. Compared to low concentrations of CytoD, a high concentration of CytoD inhibited F-actin binding to cofilin more severely

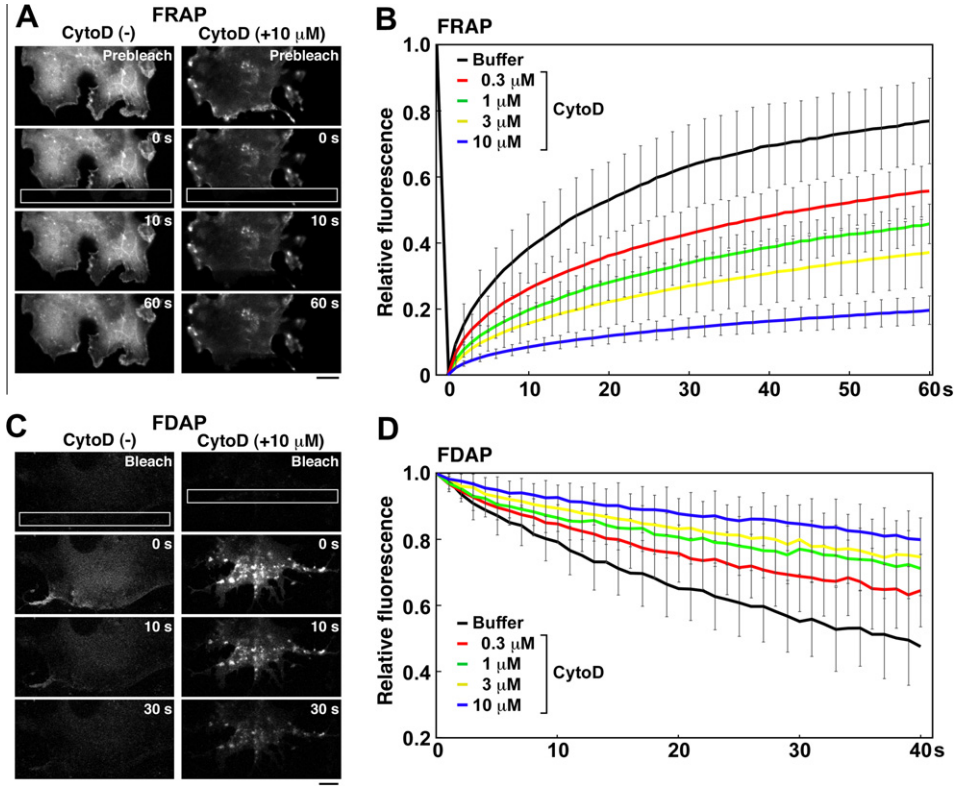

Fig. 4. CytoD decreases the rate of actin polymerization and depolymerization in cells. (A) FRAP analysis of the rate of actin polymerization. COS-7 cells expressing YFP-actin were exposed to 10 μM CytoD or control vehicle for 30 min. YFP-actin was photobleached in a rectangular region of the cell periphery (white box) and the fluorescence intensity in the photobleached region was monitored every second for 60 s. Fluorescence images at 0, 10 and 60 s after photobleaching are shown. Scale bar, 10 μm. (B) Quantification of the FRAP analysis. Data represent means ± S.D. of FRAP data from 18–20 cells. (C) FDAP analysis of the rate of actin depolymerization. COS-7 cells expressing Dronpa-actin were exposed to 10 μM CytoD or control vehicle for 30 min. After cell-wide photobleaching, Dronpa-actin was photoactivated in a rectangular region (white box) and the fluorescence intensity in the F-actin-rich area within the photoactivated region was monitored every second for 40 s. Fluorescence images at 0, 10 and 30 s after photoactivation are shown. Scale bar, 10 μm. (D) Quantification of the FDAP analysis. Data represent means ± S.D. of FDAP data from 20–24 cells.

(Fig. 2E) and increased the ratio of F-actin to total actin (Fig. 2C). Additionally, a previous study suggested that cytochalasin B may bind to actin subunits in the filaments [39,40]. These results leave open an alternative possibility that a high concentration of CytoD may bind to actin filaments along the filament length and thereby directly inhibit F-actin binding to cofilin.

FRAP and FDAP analyses revealed that CytoD decreases the rate of both actin polymerization and depolymerization. Exposure of cells to CytoD did not induce net actin polymerization or depolymerization. Thus, CytoD suppresses actin filament turnover by inhibiting both the assembly and disassembly of actin filaments. Our results indicate that CytoD inhibits binding of G- and F-actin to cofilin. Similarly, CytoD may inhibit the binding of G-actin to several G-actin-binding proteins. Therefore, CytoD affects cellular actin dynamics via multiple mechanisms, including binding to the barbed ends of actin filaments and the inhibition of the interaction between G-actin and various G-actin-binding proteins.

Acknowledgments

We thank A. Miyawaki for providing Venus and Dronpa cDNAs and T. Yamori, the Head of the Screening Committee of Anticancer Drugs, for supplying the SCADS inhibitor kits. We also thank T. Kiuchi for help on the development of the BiFC assay system. This work was supported by a grant-in-aid for Scientific Research from the Ministry of Education, Culture, Sports, Science and Technology of Japan.

References

[1] J.R. Bamburg, Proteins of the ADF/cofilin family: essential regulators of actin dynamics, Annu. Rev. Cell Dev. Biol. 15 (1999) 185–230.

[2] T.D. Pollard, G.G. Borisy, Cellular motility driven by assembly and disassembly of actin filaments, Cell 112 (2003) 453–465.

[3] M.-F. Carlier, D. Pantaloni, Control of actin assembly dynamics in cell motility, J. Biol. Chem. 282 (2007) 23005–23009.

[4] S. Ono, Mechanism of depolymerization and severing of actin filaments and its significance in cytoskeletal dynamics, Int. Rev. Cytol. 258 (2007) 1–82.

[5] N. Yang, O. Higuchi, K. Ohashi, K. Nagata, A. Wada, K. Kangawa, E. Nishida, K. Mizuno, Cofilin phosphorylation by LIM-kinase 1 and its role in Rac-mediated actin reorganization, Nature 393 (1998) 809–812.

[6] S. Arber, F.A. Barbayannis, H. Hanser, C. Schneider, C.A. Stanyon, O. Bernard, P. Caroni, Regulation of actin dynamics through phosphorylation of cofilin by LIM-kinase, Nature 393 (1998) 805–809.

[7] J. Toshima, J.Y. Toshima, T. Amano, N. Yang, S. Narumiya, K. Mizuno, Cofilin phosphorylation by protein kinase testicular protein kinase 1 and its role in integrin-mediated actin reorganization and focal adhesion formation, Mol. Biol. Cell 12 (2001) 1131–1145.

[8] R. Niwa, K. Nagata-Ohashi, M. Takeichi, K. Mizuno, T. Uemura, Control of actin reorganization by Slingshot, a family of phosphatases that dephosphorylate ADF/cofilin, Cell 108 (2002) 233–246.

[9] Y. Ohta, K. Kousaka, K. Nagata-Ohashi, K. Ohashi, A. Muramoto, Y. Shima, R. Niwa, T. Uemura, K. Mizuno, Differential activities, subcellular distribution and tissue expression patterns of three members of Slingshot family phosphatases that dephosphorylate cofilin, Genes Cells 8 (2003) 811–824.

[10] N. Yonezawa, E. Nishida, K. Iida, I. Yahara, H. Sakai, Inhibition of the interactions of cofilin, destrin, and deoxyribonuclease I with actin by phosphoinositides, J. Biol. Chem. 265 (1990) 8382–8386.

[11] L. Blanchoin, T.D. Pollard, Interaction of actin monomers with *Acanthamoeba* actophorin (ADF/cofilin) and profilin, J. Biol. Chem. 273 (1998) 25106–25111.

[12] B.W. Bernstein, J.R. Bamburg, Tropomyosin binding to F-actin protects the F-actin from disassembly by brain actin-depolymerizing factor (ADF), Cell Motil. 2 (1982) 1–8.
[13] E. Nishida, E. Muneyuki, S. Maekawa, Y. Ohta, H. Sakai, An actin-depolymerizing protein (destrin) from porcine kidney. Its action on F-actin containing or lacking tropomyosin, Biochemistry 24 (1985) 6624–6630.
[14] J.A. Cooper, Effects of cytochalasin and phalloidin on actin, J. Cell Biol. 105 (1987) 1473–1478.
[15] M.D. Flanagan, S. Lin, Cytochalasins block actin filament elongation by binding to high affinity sites associated with F-actin, J. Biol. Chem. 255 (1980) 835–838.
[16] M.-F. Carlier, P. Criquet, D. Pantaloni, E.D. Korn, Interaction of cytochalasin D with actin filaments in the presence of ADP and ATP, J. Biol. Chem. 261 (1986) 2041–2050.
[17] D.W. Goddette, C. Frieden, The binding of cytochalasin D to monomeric actin, Biochem. Biophys. Res. Commun. 128 (1985) 1087–1092.
[18] D.W. Goddette, C. Frieden, Actin polymerization. The mechanism of action of cytochalasin D, J. Biol. Chem. 261 (1986) 15974–15980.
[19] U.B. Nair, P.B. Joel, Q. Wan, S. Lowey, M.A. Rould, K.M. Trybus, Crystal structures of monomeric actin bound to cytochalasin D, J. Mol. Biol. 384 (2008) 848–864.
[20] J.F. Casella, M.D. Flanagan, S. Lin, Cytochalasin D inhibits actin polymerization and induces depolymerization of actin filaments formed during platelet shape change, Nature 293 (1981) 302–305.
[21] A. Morris, J. Tannenbaum, Cytochalasin D does not produce net depolymerization of actin filaments in HEp-2 cells, Nature 287 (1980) 637–639.
[22] K. Ohashi, T. Kiuchi, K. Shoji, K. Sampei, K. Mizuno, Visualization of cofilin-actin and Ras–Raf interactions by bimolecular fluorescence complementation assays using a new pair of split Venus fragments, Biotechniques 52 (2012) 45–50.
[23] T. Nagai, K. Ibata, E.S. Park, M. Kubota, K. Mikoshiba, A. Miyawaki, A variant of yellow fluorescent protein with fast and efficient maturation for cell-biological applications, Nat. Biotechnol. 20 (2002) 87–90.
[24] T.K. Kerppola, Visualization of molecular interactions using bimolecular fluorescence complementation analysis: characteristics of protein fragment complementation, Chem. Soc. Rev. 38 (2009) 2876–2886.
[25] M. Oikawa, T. Ueno, H. Oikawa, A. Ichihara, Total synthesis of tautomycin, J. Org. Chem. 60 (1995) 5048–5068.
[26] S. Kusumoto, M. Oikawa, Synthesis of glycolipid targets, in: B.O. Fraser-Reid, K. Tatsuta, J. Thiem (Eds.), Glycoscience. Chemistry and Chemical Biology I–III, Springer, Heidelberg, 2001, pp. 2107–2148.
[27] M. Oikawa, An improved synthesis of arylboronates toward twenty novel 1,3-disubstituted 4-amino-1H-pyrazolo[3,4-d]pyrimidine analogs, Heterocycles 81 (2010) 73–77.
[28] R. Ando, H. Mizuno, A. Miyawaki, Regulated fast nucleocytoplasmic shuttling observed by reversible protein highlighting, Science 306 (2004) 1370–1373.
[29] K. Ohashi, S. Fujiwara, T. Watanabe, H. Kondo, T. Kiuchi, M. Sato, K. Mizuno, LIM kinase has a dual role in regulating lamellipodium extension by decelerating the rate of actin retrograde flow and the rate of actin polymerization, J. Biol. Chem. 286 (2011) 36340–36351.
[30] T. Kiuchi, K. Ohashi, S. Kurita, K. Mizuno, Cofilin promotes stimulus-induced lamellipodium formation by generating an abundant supply of actin monomers, J. Cell Biol. 177 (2007) 465–476.
[31] T. Kiuchi, T. Nagai, K. Ohashi, K. Mizuno, Measurements of spatiotemporal changes in G-actin concentration reveal its effect on stimulus-induced actin assembly and lamellipodium extension, J. Cell Biol. 193 (2011) 365–380.
[32] H. Hatanaka, K. Ogura, K. Moriyama, S. Ichikawa, I. Yahara, F. Inagaki, Tertiary structure of destrin and structural similarity between two actin-regulating protein families, Cell 85 (1996) 1047–1055.
[33] P. Lappalainen, E.V. Fedorov, A.A. Fedorov, S.C. Almo, D.G. Drubin, Essential functions and actin-binding surfaces of yeast cofilin revealed by systematic mutagenesis, EMBO J. 16 (1997) 5520–5530.
[34] V.O. Paavilainen, E. Oksanen, A. Goldman, P. Lappalainen, Structure of the actin-depolymerizing factor homology domain in complex with actin, J. Cell Biol. 182 (2008) 51–59.
[35] R. Dominguez, Actin-binding proteins–a unifying hypothesis, Trends Biochem. Sci. 29 (2004) 572–578.
[36] J.S. Allingham, V.A. Klenchin, I. Rayment, Actin-targeting natural products: structures, properties and mechanisms of action, Cell. Mol. Life Sci. 63 (2006) 2119–2134.
[37] M. Hertzog, C. van Heijenoort, D. Didry, M. Gaudier, J. Coutant, B. Gigant, G. Didelot, T. Preat, M. Knossow, E. Guittet, M.-F. Carlier, The β-thymosin/WH2 domain: structural basis for the switch from inhibition to promotion of actin assembly, Cell 117 (2004) 611–623.
[38] H.Y. Kueh, G.T. Charras, T.J. Mitchison, W.M. Brieher, Actin disassembly by cofilin, coronin, and Aip1 occurs in bursts and is inhibited by barbed-end cappers, J. Cell Biol. 182 (2008) 341–353.
[39] J.H. Hartwig, T.P. Stossel, Cytochalasin B and the structure of actin gels, J. Mol. Biol. 134 (1979) 539–553.
[40] P.A. Theodoropoulos, A. Gravanis, A. Tsapara, A.N. Margioris, E. Papadogiorgaki, V. Galanopoulos, C. Stournaras, Cytochalasin B may shorten actin filaments by a mechanism independent of barbed end capping, Biochem. Pharmacol. 47 (1994) 1875–1881.